Supplementary Information (SI) for Nanoscale.

Supplementary information

Exploring Many-Body Phenomena: Biexciton Generation and Auger Recombination in Ag_2S-based Nanocrystals

Victor Vega-Mayoral,*[a,b] Saül Garcia-Orrit,[a] Peijiang Wang,[c] Rafael Morales Márquez,[c] Emma Martín Rodríguez,[d,e,f] Beatriz H. Juárez,*[c] and Juan Cabanillas-Gonzalez[a,b]

a) IMDEA Nanoscience, Faraday 9, Campus de Cantoblanco, 28049 Madrid, Spain. Email: victor.vega@imdea.org
b) Unidad de Nanomateriales Avanzados, IMDEA-Nanociencia, Unidad Asociada al CSIC por el ICMM C/ Faraday 9, 28049 Madrid, Spain.
c) Materials Science Institute of Madrid, ICMM, Spanish Research Council, CSIC, C/Sor Juana Inés de la Cruz, 3, 28049 Madrid, Spain Email: bh.juarez@csic.es
d) Departamento de Física Aplicada, Facultad de Ciencias, Universidad Autónoma de Madrid, C/Francisco Tomás y Valiente 7, Madrid, Spain
e) Instituto Ramón y Cajal de Investigación Sanitaria (IRYCIS), Ctra. Colmenar Viejo, km. 9,100, 28034 Madrid, Spain
f) Institute for Advanced Research in Chemistry (IAdChem), Campus de Cantoblanco, 28049 Madrid, Spain

Synthetic details

Chemicals

Silver (I) diethyldithiocarbamate (AgDDTC, 99%), 1-dodecanethiol (DDT, >98%), toluene (TOL, 99.8%), acetone (technical grade), oleylamine (OLA, 70%), sulfur powder (S, synthesis grade), chloroform ($CHCl_3$, >99.8%), ethanol (EtOH, 96%), selenium powder (Se, 99.99%), trioctylphosphine (TOP, 97%). All chemicals were purchased in Merck and used without further purification.

Synthesis of Ag_2S NCs by hot injection (Core Ag_2S NCs)

0.2 mmol of AgDDTC, 40 mmol of DDT and 10 ml of TOL were mixed in a three-neck round-bottom flask, connected to a Schlenk line. The mixture was heated to 100 °C until the complete dissolution of the silver salt. At this point 100 μL of a solution of 0.4 mmol of S-powder in 1 ml of OLA is swiftly injected. This solution corresponds to 0.012 ± 0.001 g of sulfur powder dissolved in 0.84 ± 0.01 g.

If just Ag_2S cores are desired, the solution is then left to react for 5 minutes and then cooled down to room temperature. When the temperature reaches approximately 60 °C, 3 mL of $CHCl_3$ is added to the sample to stop the reaction The sample is transferred into two Falcon tubes (50 mL) and precipitated by adding ethanol, sonicating for 5 min, followed by centrifugation at 9000 rpm for 10 min (one cycle). After this cycle, the sample is re-dispersed in 10 mL of $CHCl_3$.

Synthesis of $Ag_2S/Ag_2(S,Se)$ NCs (CS NCs)

In this case, after the injection of Sulphur in OLA and after 5 minutes of reaction, 100 μl of a 1 M solution of selenium, in the form of Se-powder, in TOP (prepared by dissolving 0.7894 ± 0.0001 g of Se- powder in 1.0 ± 0.1 mL of TOP) is injected into the NCs dispersion. The solution is left to react for 10 minutes, and is then cooled down to room temperature. When the temperature reaches approximately 60°C, 3 mL of $CHCl_3$ is added to the sample to stop the reaction. For purification, the NC solution is divided into 3 equal parts and added into 3 Falcon tubes (50 mL), using ethanol as non-solvent. The volume of ethanol used is approximately 2/3 of the volume of the nanoparticle dispersion in each Falcon tube. The Falcon tubes are centrifuged (9000 rpm, 10 min), and the supernatant discarded. The precipitates are collected in a total volume of 10 mL of $CHCl_3$. The average concentration of Ag measured by ICP is ~1 mg/mL of Ag.

Preparation of the Zinc-oleate stock solution

A supersaturated Zinc stock solution was prepared by mixing in a 3-neck flask 0.219 g of $Zn(Ac)_2.2H_2O$, 4.4 g OA and 4.5 g of ODE. The mixture was heated up to 130 °C for 1.5 h under vacuum. This reaction forms Zn-oleate, and the vacuum removes the produced acetic acid from the solution.[1,2] With the help of a syringe, this solution is extracted from the 3-neck flask and transferred to a vial, with a rubber cap in the cap, where air has been displaced by previously flowing N_2. The preparation of a fresh solution for each synthesis is recommended, to obtain optimized PL results of the final NCs solutions.

Synthesis of $Ag_2S/Ag_2(S,Se)$ treated with the Zn-oleate solution ($Ag_2S/ZnS/Ag_2(S,Se)$ NCs) (CSS NCs)

5 mL of the previously prepared $Ag_2S/Ag_2(S,Se)$ ~1 mg/mL NCs in $CHCl_3$ were added into a 3-neck flask, connected to the Schlenk line and heated to 60 ºC. Upon reaching this temperature, 0.25 mL of the Zn-solution (previously heated to ~80 °C) were added, and left to react for 4 minutes. After this short time, the mixture was left to cool down to room temperature (RT); thereafter, it was washed in a cycle of ethanol/chloroform, as mentioned before.

Optical characterization

UV-vis Absorption spectroscopy

Absorption spectra of NC solutions were recorded using a Cary60 (Agilent) UV-Vis spectrophotometer. Steady-state photoluminescence spectra were measured a NIR detector (Andor 1.7µm InGaAs iDus, Oxford Instruments) connected to a spectrometer (Andor Shamrock SR163, Technology, Oxford Instruments) and mounted on a fluorescence microscope (AxioVert 100, Carl Zeiss Microscopy) for the 1000-1500 nm NIR. A fiber-coupled 808 nm laser diode (LU0808M250, Lumics) is used as excitation source.

Transient Absorption Spectroscopy (TAS)

TAS spectroscopy was carried out using a femtosecond Clark-MXR CPA210 regenerative amplifier, delivering 120 fs pulses at 775 nm, with 1 kHz repetition rate. The primary beam was split into pump and probe beams. The pump pulse beam was sent to a computer-controlled delay line to shift it temporally in relation to the probe pulse; it was focused onto the sample and could be adjusted to different fluences. The probe beam was focused on a sapphire plate, to generate a supercontinuum pulse; this was spatially overlapped with the pump beam on the sample. Before impinging on the sample, a portion of the sample probe beam was split off, serving as a reference. The sample and reference probe beams were then sent to a prism spectrometer (Entwicklungsbüro Stressing, Germany) and monitored independently with two linear CCD array detectors (VIS-Enhanced InGaAs, Hamamatsu Photonics). A bespoke software synchronized the delay line setting with the signal acquisition system and recorded the normalized difference in probe intensities $\Delta T/_T$ for each individual laser pulse. Measurements were performed with pump and probe beams polarized at the so-called “magic angle” (for a brief description of the magic angle use in time-resolved fluorescence imaging, see *Ch. Buehler, C. Y. Dong, P. T. C. So, T. French and E. Gratton, Biophys. J., 2000, 79, 536–549)*. The samples in solution were enclosed in nitrogen purged cuvettes and stir in-situ with a micro stirrer to refresh the photo-pumped volume.

High-resolution transmission electron microscopy (HRTEM) images were acquired on a JEOLJEM Grand ARM 300cF microscope (Madrid, Spain), operating at 60 kV, and equipped with a Cs Corrector (ETA-JEOL) and CMOS camera (4096 x 4096 pixels, Gatan OneView).

Supporting results

Section S1. TEM images of Ag_2S Cores, CS and CSS samples

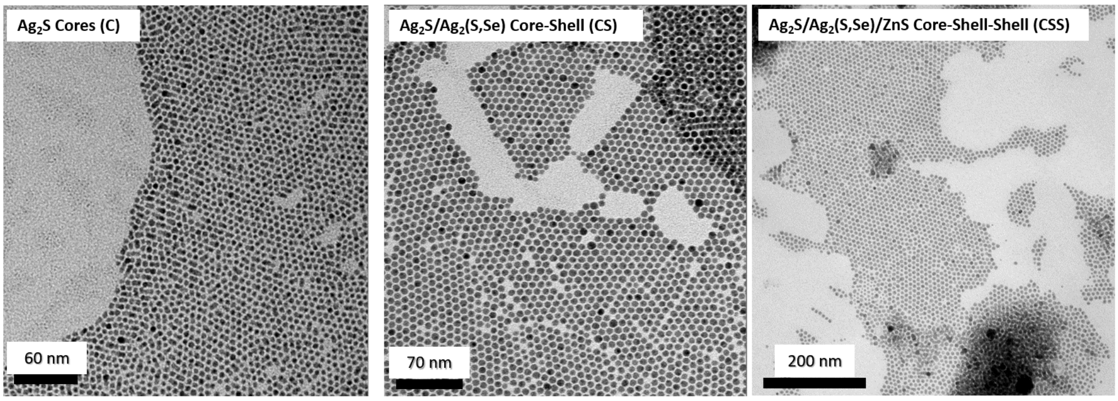

Figure S1 Low magnification TEM images of Ag_2S Cores, CS and CSS samples.

Section S2. Absorption response of Ag_2S cores with different sizes

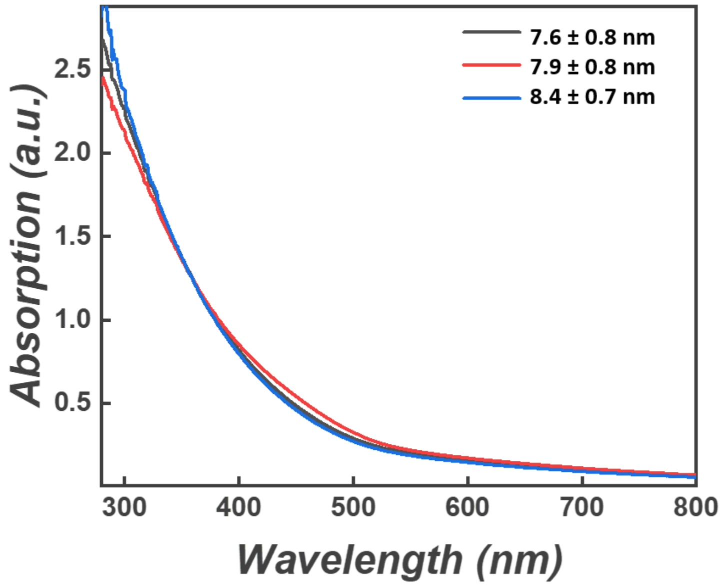

Figure S2 Absorption spectra of Ag_2S NCs with mean sizes from ~7 to 9 nm.

Section S3. Photoluminescence of Ag_2S-based nanocrystals

Normalized photoluminescence of Ag_2S-based nanocrystals has been fitted to a two Gaussian model (Figures 1 d-f, main text) using the expression:

$$I(E) = y_0 + \frac{A_1}{w_1\sqrt{\frac{\pi}{2}}} e^{-2\frac{E-E_{01}}{{w_1}^2}} \frac{A_2}{w_2\sqrt{\frac{\pi}{2}}} e^{-2\frac{E-E_{02}}{{w_2}^2}} \qquad \text{Eq. S1}$$

obtaining the following fitting parameters:

		Trapped excitons (resonance 1)	Free excitons (resonance 2)
Ag_2S NCs	y0	-0,00602 ± 8,22416E-4	-0,00602 ± 8,22416E-4
	E0	1,02269 ± 0,00125	1,0937 ± 0,00462
	w	0,10811 ± 0,00247	0,14542 ± 0,00301
	A	0,06186 ± 0,00957	0,13196 ± 0,00987
CS	y0	-0,00516 ± 9,48072E-4	-0,00516 ± 9,48072E-4
	E0	1,02563 ± 0,00174	1,09499 ± 0,00396
	w	0,09722 ± 0,00322	0,13375 ± 0,0028
	A	0,04296 ± 0,00895	0,13885 ± 0,00926
CSS	y0	-2,4419E-5 ± 6,59494E-4	-2,4419E-5 ± 6,59494E-4
	E0	1,01828 ± 9,12406E-4	1,10255 ± 8,54309E-4
	w	0,08741 ± 0,00212	0,13961 ± 8,68047E-4
	A	0,01855 ± 0,00192	0,17016 ± 0,00213

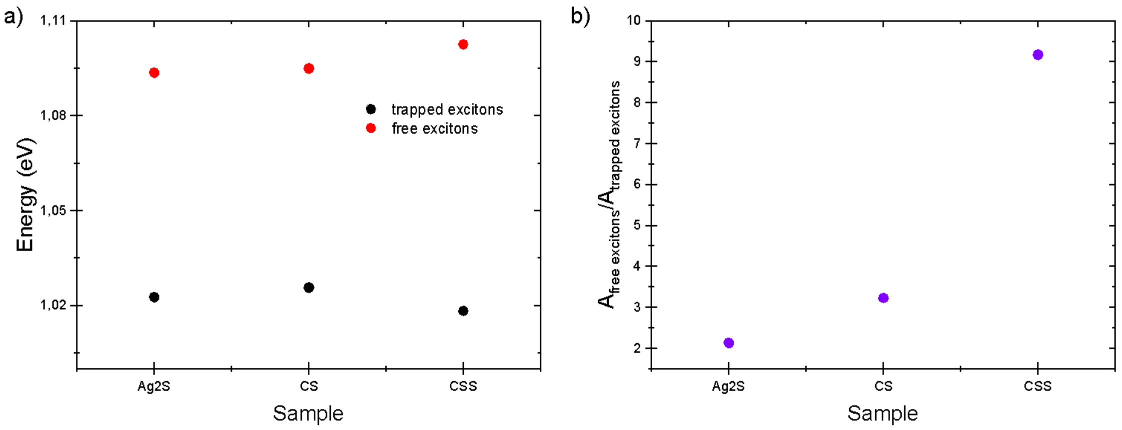

Figure S3 a) Central position of peaks assigned to contributions to the photoluminescence from free excitons (red dots) and trapped excitons (black dots), and b) ratio of the intensities of the two peaks from the PL spectra shown in Figure 1d-f.

Section S4. Estimation of bulk and surface defects in Ag_2S plain cores and passivated $Ag_2S/Ag_2(S,Se)/ZnS$ CSS NCs.

We can make a calculation based on the known PLQY of the samples. The plain Ag_2S cores exhibit PLQY 1% while passivated core-shell-shell CSS structures show a PLQY≈10%.

The PLQY is defined as: (1)

$$PLQY = \frac{K_r}{K_r + K_{nr}}$$

Where K_r is the radiative recombination rate and K_{nr} the non-radiative one. We can reorganize the above expression to: (2)

$$K_{nr} = K_r\left(\frac{1}{PLQY} - 1\right)$$

The non-radiative paths will include both surface defects ($D_{surface}$) and bulk defects (D_{bulk}) so we can say that the non-radiative rate will have contributions both from surface and bulk: (3)

$$K_{nr} = k_{bulk} + K_{surface}$$

However, tor CSS samples (passivated surface) we can assume that $K_{surface}$ does not contribute and therefore: (4)

$$K_{nr(CSS)} = k_{bulk}$$

And therefore, taking expression (2) into account, for CSS NCs: (5)

$$K_{bulk} = K_r\left(\frac{1}{PLQY\ (CSS)} - 1\right)$$

For the Ag$_2$S plain cores, with no passivation we must say: (6)

$$K_{bulk} + K_{surface} = K_r\left(\frac{1}{PLQY\ (plain\ cores)} - 1\right)$$

From these expressions we can conclude that: (7)

$$K_{surface} = K_r\left[\left(\frac{1}{PLQY\ (plain\ cores)} - 1\right) - \left(\frac{1}{PLQY\ (CSS)} - 1\right)\right]$$

Substituting PLQY (CSS)= 0.1 (10%) and PLQY (cores)= 0.01 (1%)we get: (8)

$$K_{surface} = K_r\left[\left(\frac{1}{0.01}\right) - \left(\frac{1}{0.1}\right)\right] = 90K_r$$

Substituting in expression (2) for CSS samples and plain cores, we get:

For Plain Ag$_2$S cores:

$$K_{nr} = K_r\left(\frac{1}{0.01} - 1\right) = K_r(100 - 1) = 99K_r$$

For CSS passivated nanocrystals:

$$K_{nr} = K_r\left(\frac{1}{0.10} - 1\right) = K_r(10 - 1) = 9K_r$$

The portion of surface and bulk defects, the $D_{surface}$ and D_{bulk} in non-radiative paths can be expressed as in the following expressions, (9) and (10)

$$D_{bulk} = \frac{k_{bulk}}{K_{bulk}+K_{surface}} \qquad D_{surface} = \frac{k_{surface}}{K_{bulk}+K_{surface}}$$

Where $K_{bulk} + K_{surface}$ are rate constants of non-radiative paths related to bulk and surface, respectively.

Substituting in (9) and (10)

$$D_{bulk} = \frac{9_{Kr}}{9_{Kr} + 90K_r} \approx 9.1\%$$

$$D_{surface} = \frac{90_{Kr}}{9_{Kr} + 90K_r} \approx 90.9\%$$

This means that for Ag_2S plain cores, around 90.9% of non-radiative paths are due to surface defects, while around 9% is due to bulk defects. Since the cores are identical in CS and CSS samples (*i.e*, we used the plain Ag_2S cores for growing the shell), it can be deduced that the amount of defects in all structures related to bulk is around 9%.

Section S5. Identifying the reaction order

A first order kinetic evolution follows the differential equation:

$$\frac{dA}{d\tau} = -kA \qquad \text{Eq S2}$$

Where A is the population of a certain photoexcited state and k is the decay rate and τ is the temporal delay. This differential equation can be easily integrated to the following exponential expression:

$$A = A_0 + Be^{-k\tau} \qquad \text{Eq S3}$$

A first order kinetic evolution is identified by a linear relationship between log(A) and delay. Second order reactions follow a temporal evolution given by Eq. S4:

$$\frac{dA}{d\tau} = -kA^2 \qquad \text{Eq S4}$$

Equation S4 can be rearranged as

$$\frac{dA}{A^2} = -kd\tau \qquad \text{Eq S5}$$

Equation S5 can be integrated, obtaining the integrated dynamic equation:

$$\frac{1}{A(\tau)} = k\tau + \frac{1}{A_0} \qquad \text{Eq S6}$$

A second order kinetic evolution is then, in agreement with Equation S6, identified by a linear dependence between $\frac{1}{A}$ and τ. As mentioned in the main manuscript we have found such dependence in our Ag_2S-based nanocrystals and is represented on Figure S3 for 0.9 eV photon energy temporal trace. The dashed orange lines have been included in the figures to guide the eye.

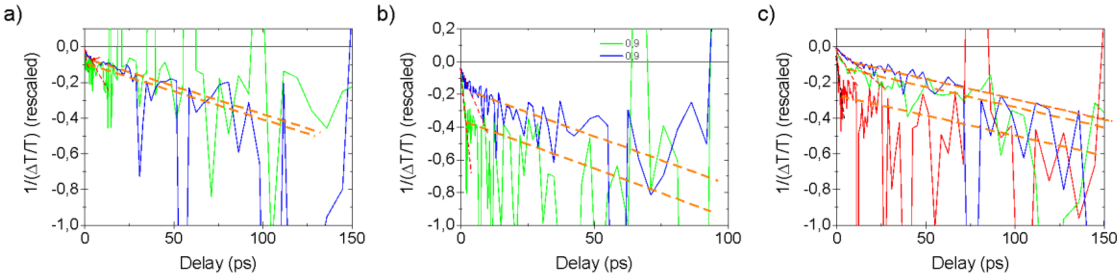

Figure S4 $\frac{1}{\frac{\Delta T}{T}}$ for (a) Ag_2S NCs, (b) CS and (c) CSS. Red lines correspond to measurements performed pumping with 0.32(red), 0.6 (green) and 1.29 (blue) mJ/cm^2. Red dashed lines have been added to guide the eye.

Section S6. Modelling TAS measurements

Global fit analysis has been used to fit transient absorption measurements. When the samples are pumped with 0.16 mJ/cm^2 the following model is used to describe the system:

$$\frac{dE_1}{dt} = G - k_1E_1 \qquad \text{Eq7}$$
$$\frac{dE_2}{dt} = k_1E_1 - k_2E_2 \qquad \text{Eq8}$$

At higher fluence the goodness of the fit worsens and, in agreement with spectra and temporal trace analysis, the following model is proposed.

$$\frac{dE_1}{dt} = G - k_1E_1 \qquad \text{Eq9}$$
$$\frac{dE_2}{dt} = k_1E_1 - \gamma_2{E_2}^2 \qquad \text{Eq10}$$
$$\frac{dE_3}{dt} = \gamma_2{E_2}^2 - \gamma_3{E_3}^2 \qquad \text{Eq11}$$
$$\frac{dE_4}{dt} = \gamma_3{E_3}^2 - k_4E_4 \qquad \text{Eq12}$$

Note that a quadratic Auger recombination implies assuming excitons as the interacting particles, since free carrier Auger recombination has a cubic dependence.

Comparison of TAS data with Global Fit Analysis (GFA)

The following images are shown to compare the transient absorption data (left images) and the output of the global fit analysis (right images), of all samples (plain Ag_2S C, CS, and CSS at both pump photon energies 1.6 and 3.2 eV and at the chosen pump fluences (the measurements pumped with 0.16 mJ/cm^2 have been fitted with the model described by Eqs 7 and 8, while for measurements pumped with 0.32, 0.6, 1.29 mJ/cm^2 fluences the model is given by Eqs 9-12)

Ag_2S plain nanocrystal cores

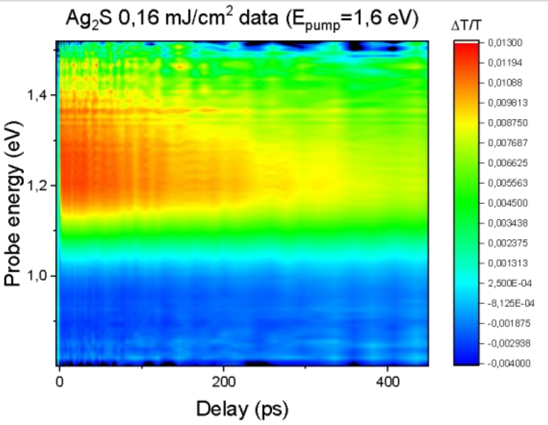

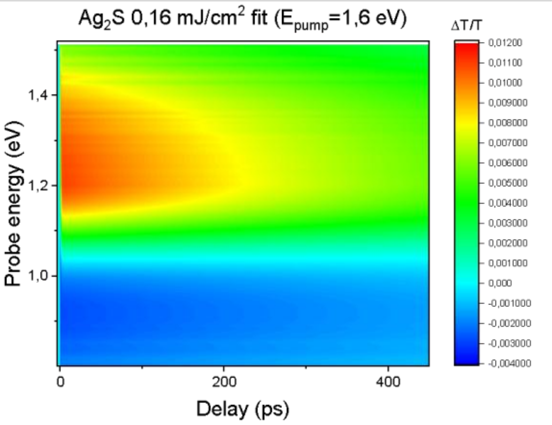

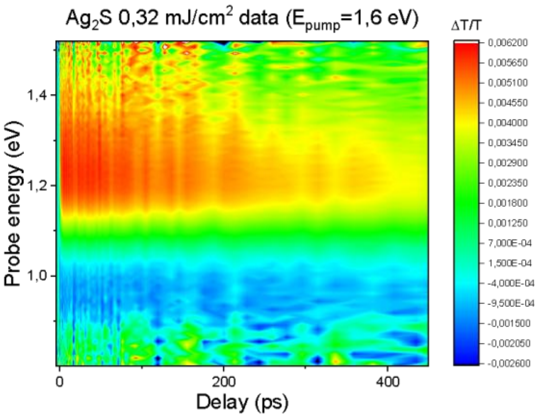

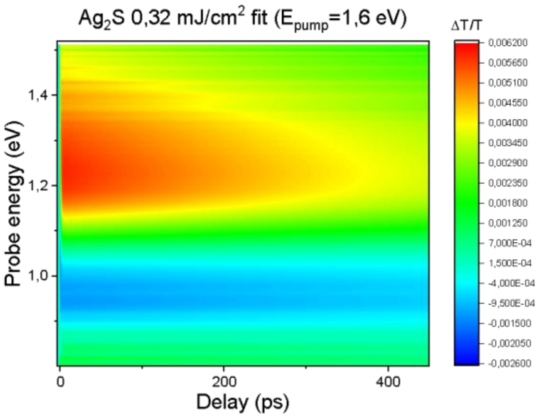

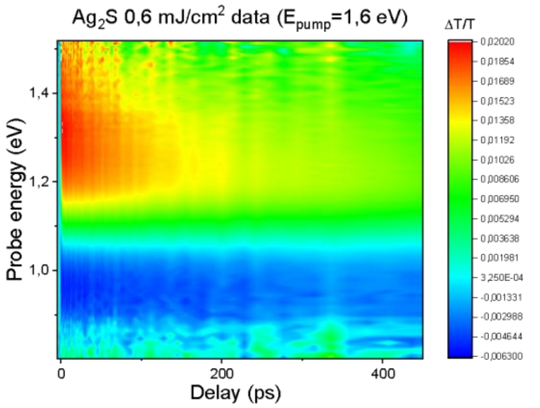

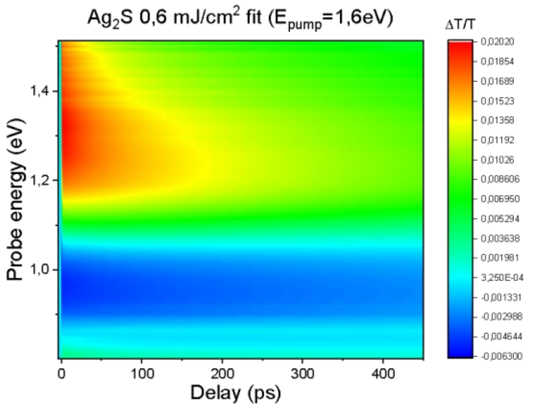

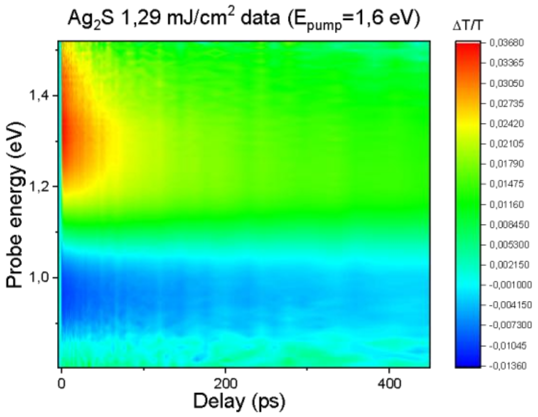
Ag_2S 1,29 mJ/cm^2 data (E_{pump}=1,6 eV)

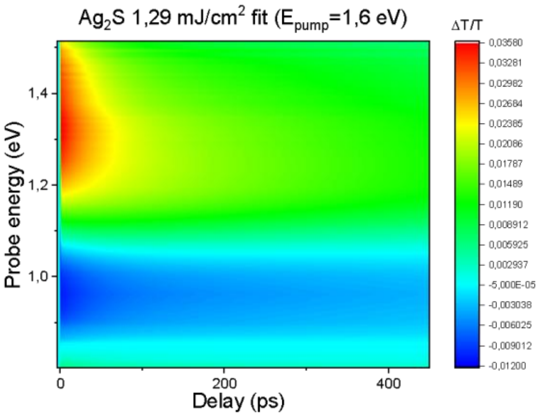
Ag_2S 1,29 mJ/cm^2 fit (E_{pump}=1,6 eV)

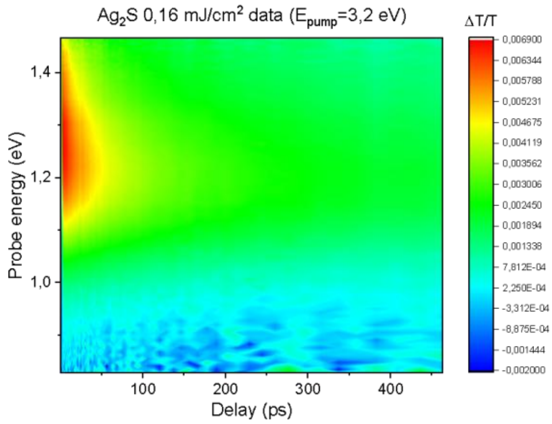
Ag_2S 0,16 mJ/cm^2 data (E_{pump}=3,2 eV)

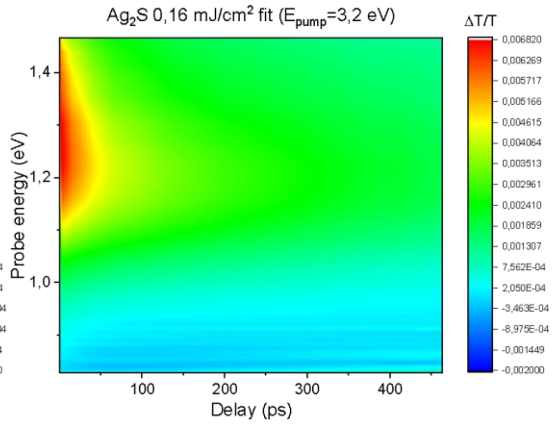
Ag_2S 0,16 mJ/cm^2 fit (E_{pump}=3,2 eV)

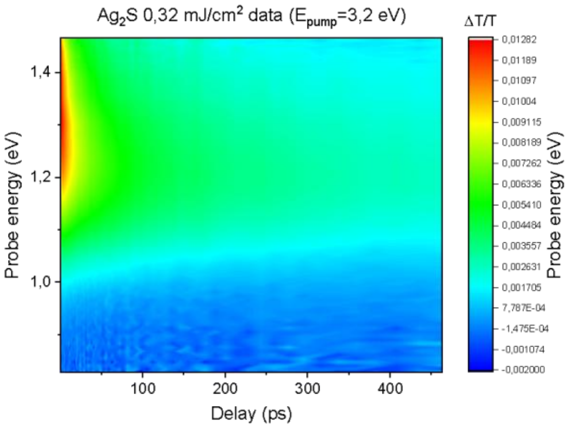
Ag_2S 0,32 mJ/cm^2 data (E_{pump}=3,2 eV)

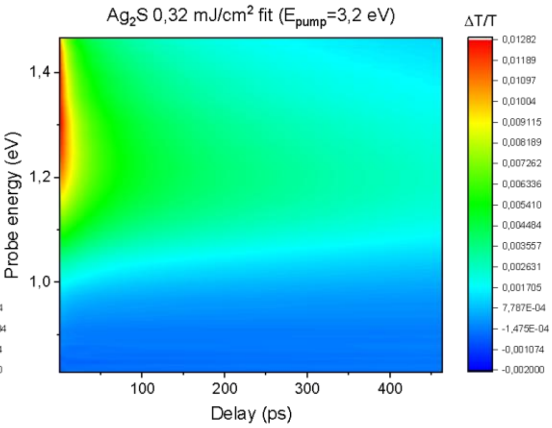
Ag_2S 0,32 mJ/cm^2 fit (E_{pump}=3,2 eV)

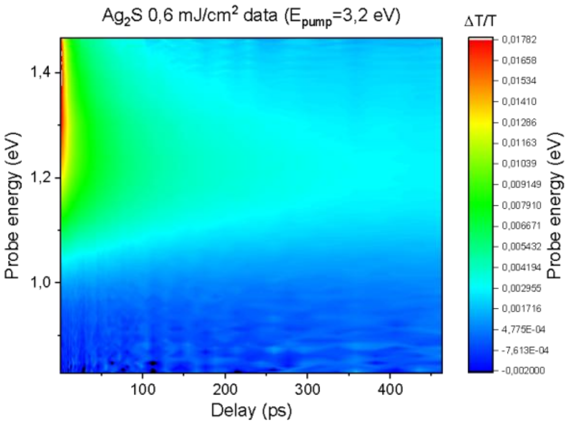
Ag_2S 0,6 mJ/cm^2 data (E_{pump}=3,2 eV)

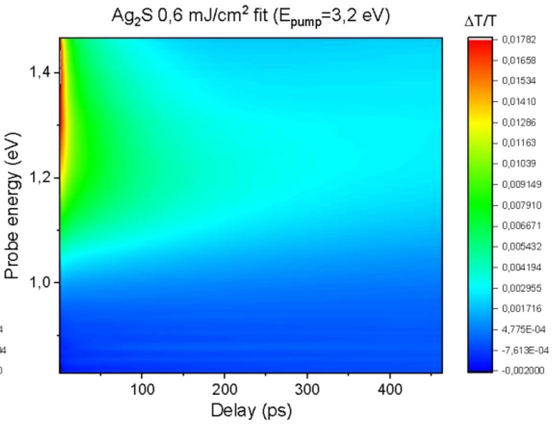
Ag_2S 0,6 mJ/cm^2 fit (E_{pump}=3,2 eV)

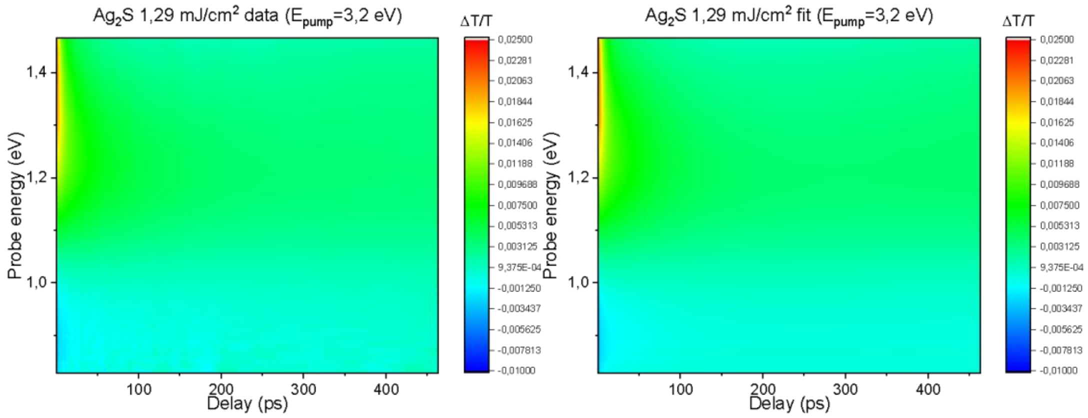

The fitting procedure applied to Ag_2S C NCs provided us with τ_1=840 fs and τ_2=944 ps as lifetimes for the 0,16 mJ/cm^2 measurement and with τ_1=500 fs, $\gamma_2 = 1.89\ 10^{-4}$ fs^{-1}cm^{-3}, $\gamma_3 = 1.94\ 10^{-5}$ and τ_2 =517 ps for high fluence measurements (0.32, 0.6, 1.29 mJ/cm^2) and 3.2 eV as energy of pump photons.

$Ag_2S/Ag_2(S,Se)$ CS nanocrystals

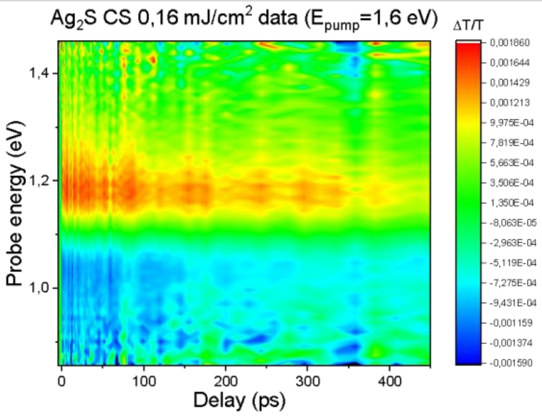
Ag_2S CS 0,16 mJ/cm^2 data (E_{pump}=1,6 eV)

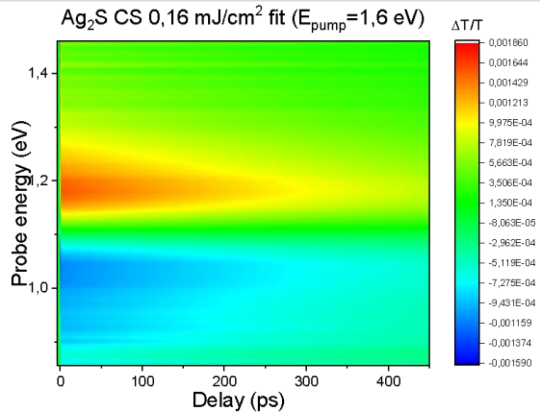
Ag_2S CS 0,16 mJ/cm^2 fit (E_{pump}=1,6 eV)

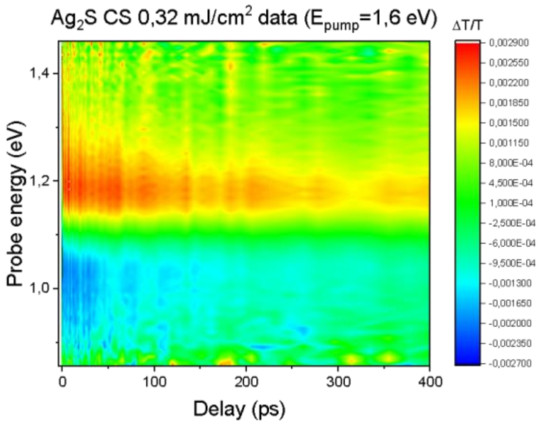
Ag_2S CS 0,32 mJ/cm^2 data (E_{pump}=1,6 eV)

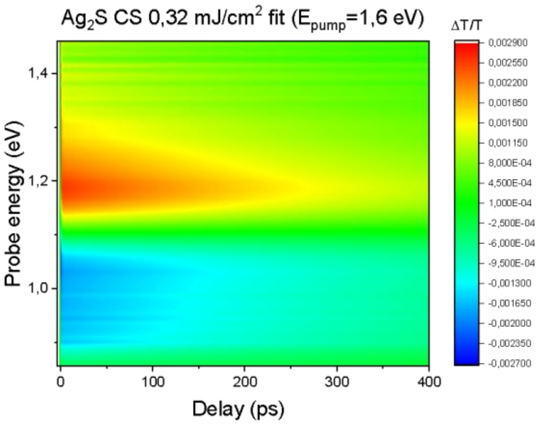
Ag_2S CS 0,32 mJ/cm^2 fit (E_{pump}=1,6 eV)

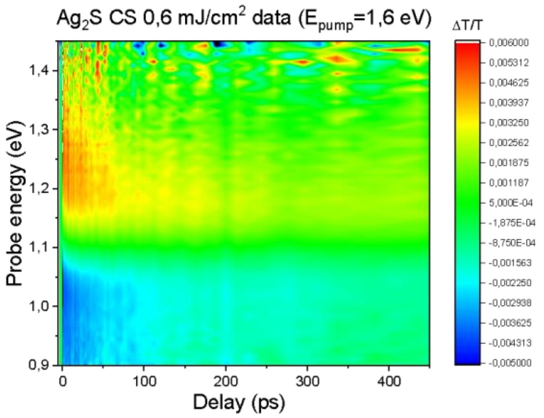
Ag_2S CS 0,6 mJ/cm^2 data (E_{pump}=1,6 eV)

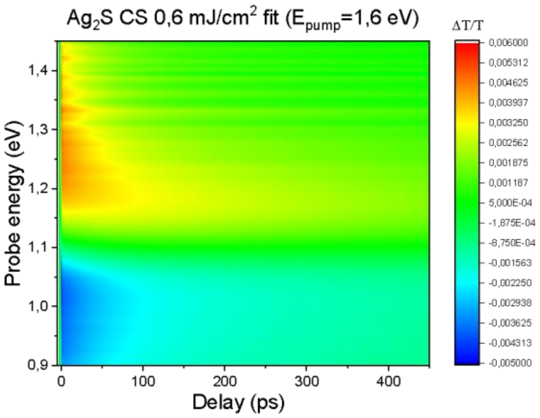
Ag_2S CS 0,6 mJ/cm^2 fit (E_{pump}=1,6 eV)

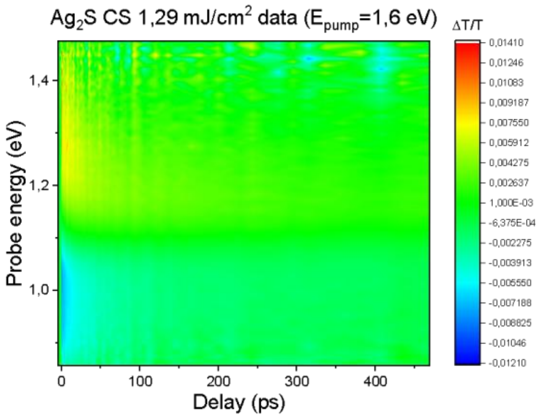
Ag_2S CS 1,29 mJ/cm^2 data (E_{pump}=1,6 eV)

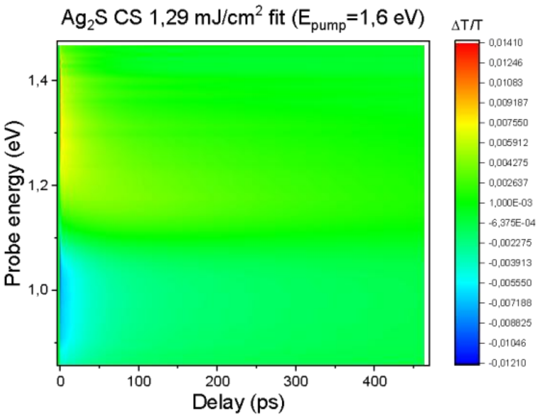
Ag_2S CS 1,29 mJ/cm^2 fit (E_{pump}=1,6 eV)

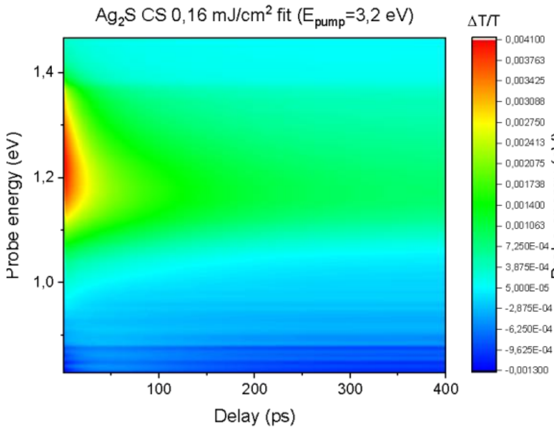
Ag_2S CS 0,16 mJ/cm^2 fit (E_{pump}=3,2 eV)

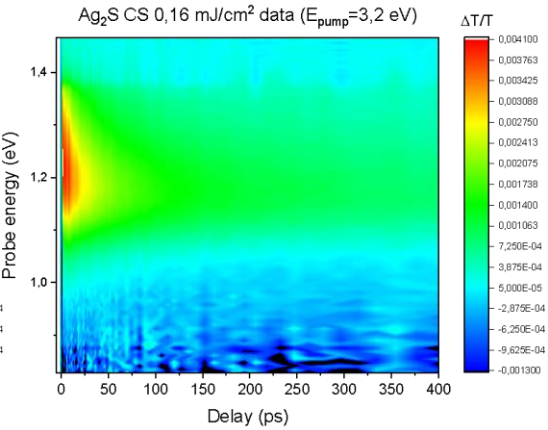
Ag_2S CS 0,16 mJ/cm^2 data (E_{pump}=3,2 eV)

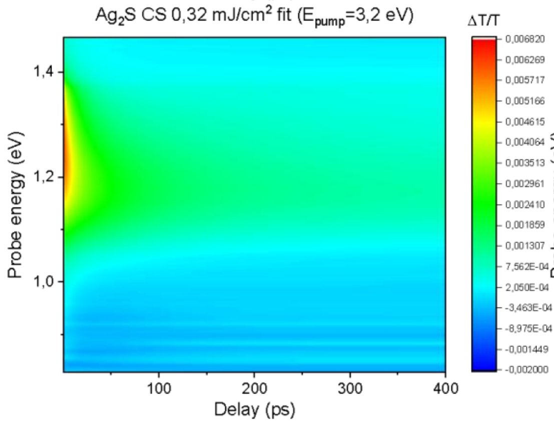
Ag_2S CS 0,32 mJ/cm^2 fit (E_{pump}=3,2 eV)

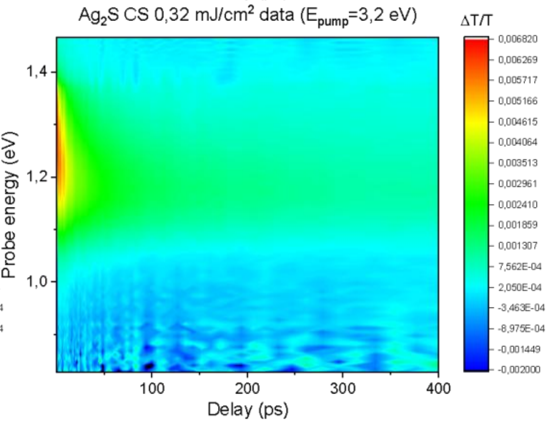
Ag_2S CS 0,32 mJ/cm^2 data (E_{pump}=3,2 eV)

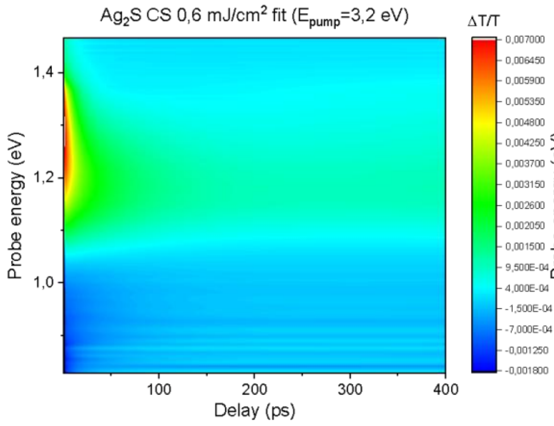
Ag_2S CS 0,6 mJ/cm^2 fit (E_{pump}=3,2 eV)

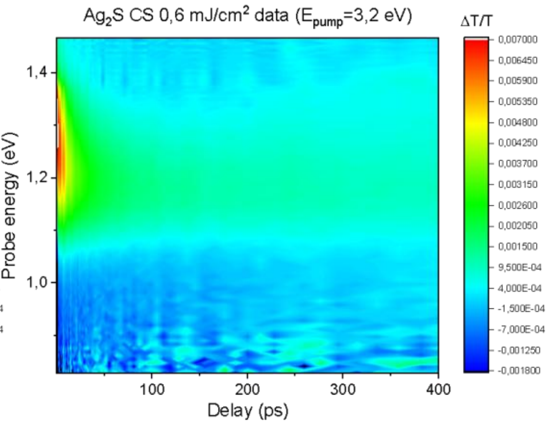
Ag_2S CS 0,6 mJ/cm^2 data (E_{pump}=3,2 eV)

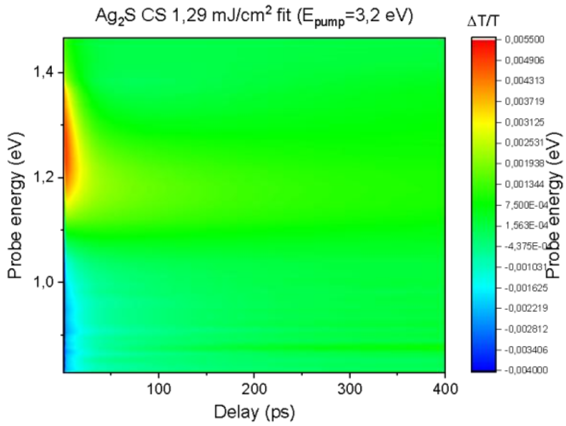
Ag_2S CS 1,29 mJ/cm^2 fit (E_{pump}=3,2 eV)

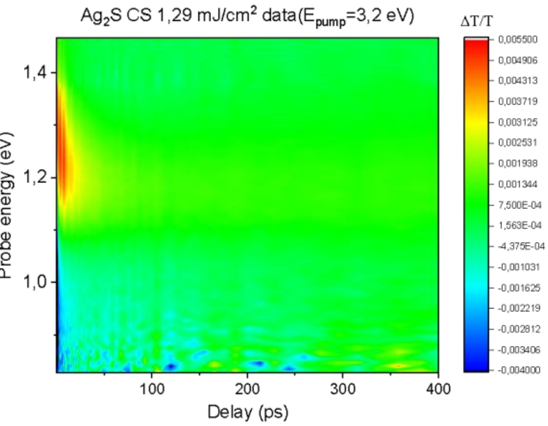
Ag_2S CS 1,29 mJ/cm^2 data(E_{pump}=3,2 eV)

The fitting procedure applied to Ag_2S CS NCs provided us with τ_1=240 fs and τ_2=649 ps as lifetimes for the 0,16 mJ/cm^2 measurement and with τ_1=294 fs, $\gamma_2 = 4.36\ 10^{-4}$ fs^{-1}cm^{-3}, $\gamma_3 = 6.32\ 10^{-5}$ and τ_2 =475 ps for high fluence measurements (0.32, 0.6, 1.29 mJ/cm^2) and 3.2 eV as energy of pump photons. Be aware that these values might be affected by the reduced photostability of Ag_2S CS nanocrystals. If the output of the fit is accepted, the lifetimes and rate constants have intermediate values between the C and CS samples.

$Ag_2S/Ag_2(S,Se)/ZnS$ CSS nanocrystals

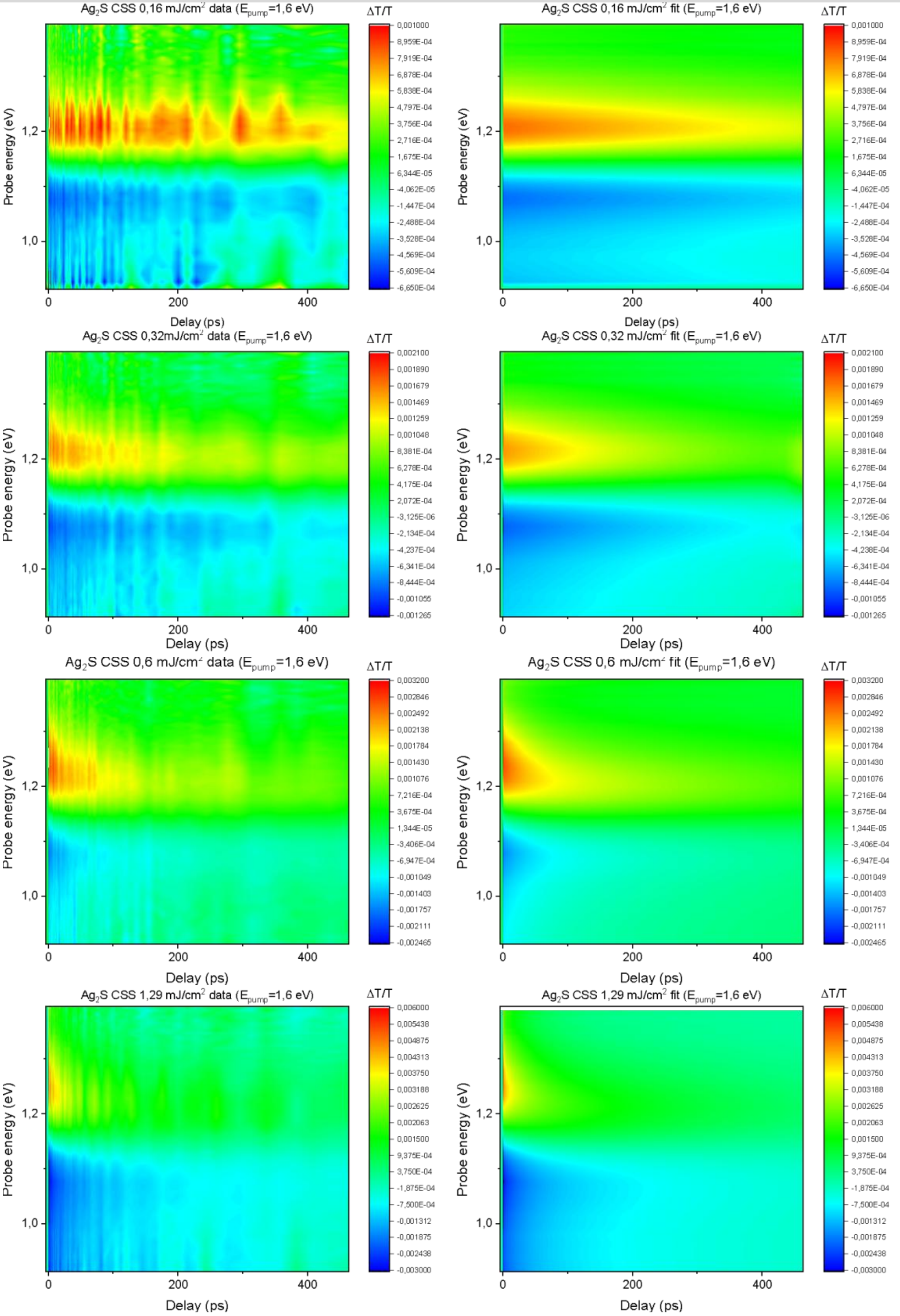

Ag$_2$S CSS 0,16 mJ/cm^2 data (E$_{pump}$=3,2 eV)

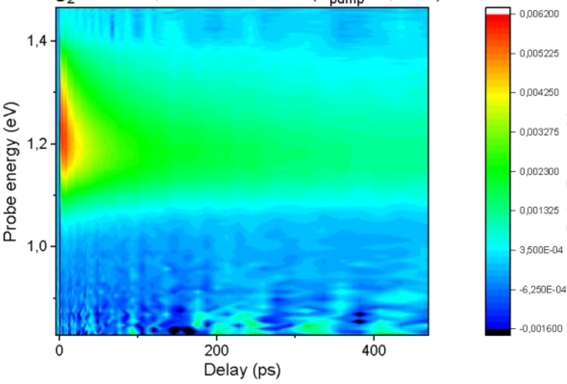

Ag$_2$S CSS 0,16 mJ/cm^2 fit (E$_{pump}$=3,2 eV)

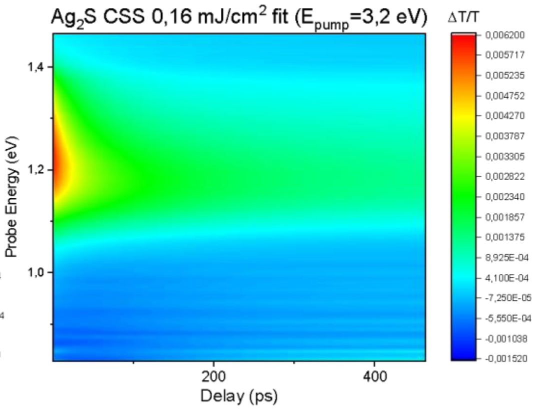

Ag$_2$S CSS 0,32 mJ/cm2 data (Epump=3,2 eV)

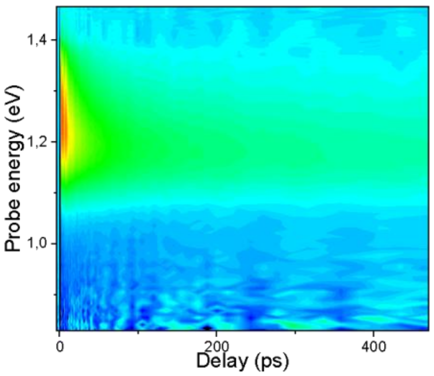

Ag$_2$S CSS 0,32 mJ/cm2 data (Epump=3,2 eV)

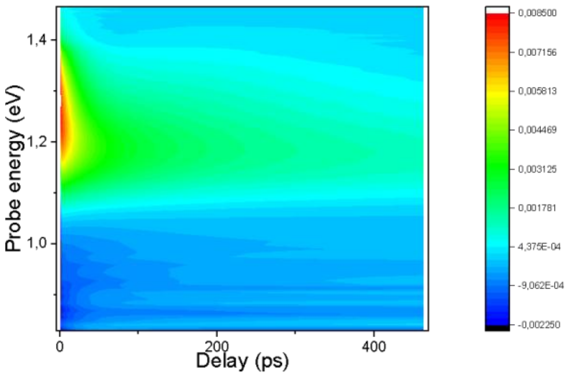

Ag$_2$S CSS 0,6 mJ/cm^2 data (E$_{pump}$=3,2 eV)

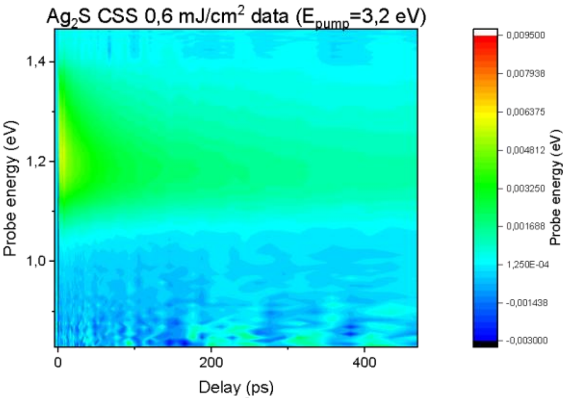

Ag$_2$S CSS 0,6 mJ/cm^2 fit (E$_{pump}$=3,2 eV)

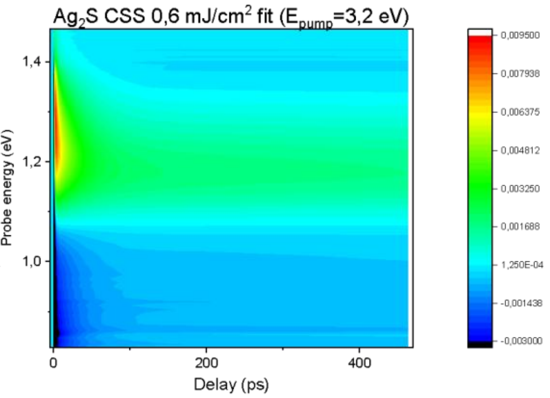

Ag$_2$S CSS 1,29 mJ/cm^2 data (E$_{pump}$=3,2 eV)

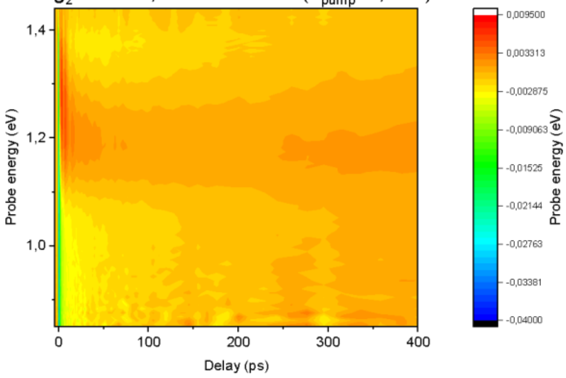

Ag$_2$S CSS 1,29 mJ/cm^2 fit (E$_{pump}$=3,2 eV)

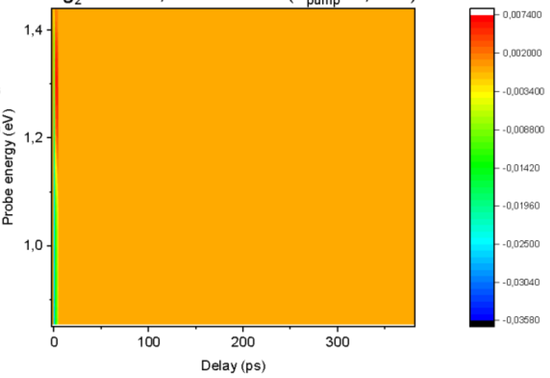

The fitting procedure applied to Ag$_2$S CSS NCs provided us with τ$_1$=243 fs and τ$_2$=1043 ps as lifetimes for the 0,16 mJ/cm^2 measurement and with τ$_1$=355 fs, $\gamma_2 = 9.9\ 10^{-4}$ fs^{-1}cm^{-3}, $\gamma_3 = 6.7\ 10^{-5}$ and τ$_2$ =166 ps for high fluence measurements (0.32, 0.6, 1.29 mJ/cm^2) and 3.2 eV as energy of pump photons.